FULL PAPER
THE ANALYST
www.rsc.org/analyst

Electrochemiluminescence of tris(2,2′-bipyridine)ruthenium(II) immobilized in poly(*p*-styrenesulfonate)–silica–Triton X-100 composite thin-films

Haiyan Wang, Guobao Xu and Shaojun Dong*

Laboratory of Electroanalytical Chemistry, Changchun Institute of Applied Chemistry, Chinese Academy of Sciences, Changchun, Jilin, 130022, China. E-mail: dongsj@ns.ciac.jl.cn

Received 9th January 2001, Accepted 18th April 2001
First published as an Advance Article on the web 21st June 2001

The electrochemiluminescence (ECL) of tris(2,2′-bipyridine)ruthenium(II) [$Ru(bpy)_3^{2+}$] immobilized in poly(*p*-styrenesulfonate) (PSS)–silica–Triton X-100 composite films was investigated. The cooperative action of PSS, sol–gel and Triton X-100 attached $Ru(bpy)_3^{2+}$ to the electrode strongly, and the presence of Triton X-100 prevented drying fractures of the sol–gel films during gelation and even on repeated wet–dry cycles. The modified electrode was used for the ECL detection of oxalate, tripropylamine (TPA) and NADH in a flow injection analysis (FIA) system with a newly designed flow cell. The detection scheme exhibited good stability, short response time and high sensitivity. Detection limits were 0.1, 0.1 and 0.5 μmol L^{-1} for oxalate, TPA and NADH, respectively, and the linear concentration range extended from 0.001 to 1 mmol L^{-1} for the three analytes. Applications of the flow cell in ECL and electrochemical detection, as well as the immobilization of reagents based on the cooperative action, are suggested.

Introduction

The electrochemiluminescence (ECL) of tris(2,2′-bipyridine)-ruthenium(II) [$Ru(bpy)_3^{2+}$] has received great attention due to its excellent intrinsic characteristics.[1–6] It has been used extensively in chemical analysis as a sensitive detection method for numerous analytes such as oxalate,[1,2,7,8] NADH,[9,10] amines,[11–13] and amino acids.[14,15] However, analytes are usually detected using solution-phase $Ru(bpy)_3^{2+}$ ECL and the continuous delivery of $Ru(bpy)_3^{2+}$ into the reaction zone is required, which limits the widespread application of $Ru(bpy)_3^{2+}$ ECL. One approach to overcome this limitation is to immobilize $Ru(bpy)_3^{2+}$ on an electrode surface.[16]

Several methods have been developed to immobilize $Ru(bpy)_3^{2+}$ on an electrode surface.[9,16-20] Bard's group has immobilized $Ru(bpy)_3^{2+}$ onto an electrode by forming Langmuir–Blodgett[17,18] and self-assembled films[19,20] of the derivatives of $Ru(bpy)_3^{2+}$. However, the Langmuir–Blodgett films are easily washed from the electrode with chloroform[17] and the self-assembled films are unstable during the potential scan.[20] Nieman and co-workers[9,16] have immobilized $Ru(bpy)_3^{2+}$ in Nafion films, but the Nafion film suffers from slow mass transfer through the film and the partitioning of $Ru(bpy)_3^{2+}$ into the more hydrophobic regions of Nafion.[9]

SiO_2-based gels are attractive matrices for the incorporation of chromophoric materials[21-23] due to their excellent physical and chemical stability and the ease with which the silica gels can be prepared.[23] Dvorak and DeArmond[24] first reported that $Ru(bpy)_3^{2+}$ incorporated into SiO_2 sol–gels on the surfaces of Pt and indium–tin oxide (ITO) have well-defined electron transfer and excited-state properties; however, the diffusion loss of $Ru(bpy)_3^{2+}$ into external solutions occurs. To overcome this problem, Khramov and Collinson[25] have immobilized $Ru(bpy)_3^{2+}$ into Nafion–silica composite films. While the resulting electrode shows improved reactivity, it needs to be kept in a high-humidity environment and the partitioning of $Ru(bpy)_3^{2+}$ into the more hydrophobic regions of Nafion still occurs.

It has been reported that polyelectrolyte-containing silica composites are highly ion-exchangeable while retaining the nanoscale porosity and optical transparency of the parent sol–gel glass.[26] In this paper, we report the first attempt to immobilize $Ru(bpy)_3^{2+}$ in poly(*p*-styrenesulfonate) (PSS)–silica–Triton X-100 composite films onto glassy carbon electrode (GCE) surfaces. The analytical performance of the modified electrode was evaluated in a flow injection analysis (FIA) system with a new flow cell. The as-prepared electrode showed good stability due to the strong interaction between $Ru(bpy)_3^{2+}$ and the composite films, and the prevention of drying fractures of the sol–gel films by Triton X-100.[27] Meanwhile, the analytes studied were determined with high sensitivity and short response time, which was attributed to the greater accessibility of the redox site and/or the faster partitioning of reagents into the films.

Experimental

Chemicals

Tris(2,2′-bipyridyl)dichlororuthenium hexahydrate [$Ru(bpy)_3Cl_2{\cdot}6H_2O$], tripropylamine (TPA), PSS and tetraethoxysilane (TEOS) were purchased from Aldrich and were used as received. All other reagents were of reagent-grade. Solutions were prepared with water purified in a Millipore system.

Instrumentation

Electrochemical measurements were performed in a conventional three-electrode cell (volume 0.8 mL) with a CHI 600 Voltammetric Analyzer. The working electrode was the $Ru(bpy)_3^{2+}$-modified GCE with a Pt wire electrode as the counter electrode and Ag/AgCl (sat. KCl) as the reference electrode. All potentials were measured and reported with respect to the Ag/AgCl (sat. KCl) reference electrode.

The FIA system used was described in a previous study.[28] A peristaltic pump was used to deliver the buffered carrier stream. The injection valve was equipped with an injection loop of 50 μL for delivery of the solutions containing the analyte. ECL

intensities were measured through the bottom of the flow cell with a BPCL Ultra-Weak Luminescence Analyzer, which was purchased from the Institute of Biophysics, Chinese Academy of Sciences. The photomultiplier tube (PMT) used in the BPCL Ultra-Weak Luminescence Analyzer was operated in current mode. Unless noted otherwise, the PMT was biased at 800 V.

A diagram of the flow cell used in the FIA system is shown in Fig. 1. Two Teflon spacers (thickness: 50 μm) were sandwiched between the electrode block and the Plexiglas window, creating a 24 μL flow cell volume which was determined by evaluating the volume of the cavity between the electrode block and the Plexiglas window from the sample inlet to the electrode. The working electrode was fixed through a hollow screw. Silicone and Teflon gaskets were used to avoid the rotation of the working electrode and to protect the Teflon spacers. The other function of the silicone gasket was to avoid leakage of the solution. An Ag/AgCl reference electrode and a Pt wire counter electrode were attached to the outlet of the flow cell.

Flow injection analysis (FIA)

The carrier stream was 0.1 mol L^{-1} phosphate buffer. The flow rate was 1.27 mL min^{-1}. In the flow cell, the solution was controlled to flow in a certain direction, which is marked by the solid arrows in Fig. 1. When the solution approached the electrode, the f1ow direction had to be changed and the solution flowed to the electrode vertically, probably being 'jetted' onto the electrode surface, which allowed the analytes to reach the electrode surface quickly.

Fabrication of the modified electrode

The procedure for immobilizing $Ru(bpy)_3^{2+}$ on to the GCE was briefly as follows: the GCE (area: 0.126 cm^2) was polished with 1 and 0.3 μm α-alumina slurry, respectively, rinsed thoroughly with water between each polishing step, sonicated in ethanol and water successively and then allowed to dry at room temperature.

The silica sols were prepared as previously described.[29] In brief, TEOS was mixed with water, ethanol, 0.1 mol L^{-1} HCl and Triton X-100. The mixture was sonicated for approximately 1 h until a clear and homogeneous solution resulted and was subsequently stored at room temperature for 2–3 h.

The ion-association complex between $Ru(bpy)_3^{2+}$ and PSS was formed by mixing an aqueous solution of $Ru(bpy)_3^{2+}$ with PSS in the desired volume ratio, while the content of $Ru(bpy)_3^{2+}$ remained constant. An orange precipitate was generated. Absolute ethanol was added to the mixture until the precipitate was dissolved, and a clear and homogeneous solution was obtained, and the volume of the solution was kept constant with absolute ethanol. Silica sol was blended with the resulting solution in a volume ratio of 2:3. An aliquot (5 μL) of the mixture solution thus obtained was then dropped onto the GCE surface and allowed to dry in the dark for 18 h. The amount of $Ru(bpy)_3^{2+}$ for all the modified electrodes was about 6.4×10^{-5} mg. All the modified electrodes were washed thoroughly with water and stored in a dry state.

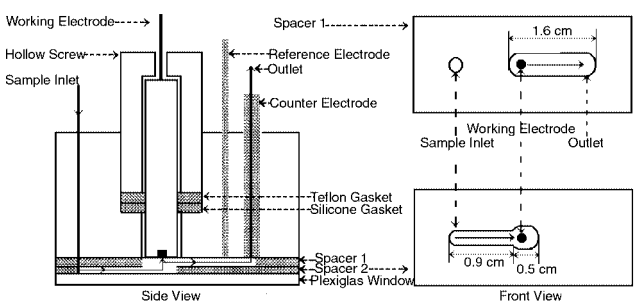

Fig. 1 Diagram of the flow cell.

Results and discussion

Electrochemistry and ECL of immobilized $Ru(bpy)_3^{2+}$

Since the $Ru(bpy)_3^{2+}$–TPA system has been well studied and shown to give rise to *ca*. 10-fold higher ECL compared with other commonly used co-reactants such as oxalate,[11,12] it was decided to use this system to examine the cyclic voltammograms (CVs) and the ECL of $Ru(bpy)_3^{2+}$ immobilized in the PSS–silica composite films.

Fig. 2 shows the CVs of $Ru(bpy)_3^{2+}$ immobilized in a 16.7% PSS–silica composite film in 0.1 mol L^{-1} phosphate buffer (pH 7.0) at various scan rates. A pair of redox waves appeared with an oxidation peak at 1.1 V and a reduction peak at 1.0 V, which was attributed to the one-electron redox reaction of $Ru(bpy)_3^{2+}$. In addition, the surface coverage of the immobilized $Ru(bpy)_3^{2+}$ was estimated to be 2×10^{-9} mol cm^{-2} from the CV at low scan rate. The oxidation peak current was proportional to the square root of the scan rate in the range 10–100 mV s^{-1} (inset in Fig. 2), while at higher scan rates, a noticeable deviation from linearity was observed. The charge transport diffusion coefficient of $Ru(bpy)_3^{2+}$ immobilized in a 16.7% PSS–silica composite film was estimated to be 5.9×10^{-10} cm^2 s^{-1} by using the Randles–Sevcik equation.

Fig. 3A depicts the CVs of $Ru(bpy)_3^{2+}$ immobilized in a 50% PSS–silica composite film acquired at 10 mV s^{-1} in 0.1 mol L^{-1} phosphate buffer (pH 7.0) with and without TPA. In the presence of TPA, the anodic current increased dramatically due to the reaction between $Ru(bpy)_3^{2+}$ and TPA. At higher scan rates, *e.g*., 100 mV s^{-1}, the changes in the CV curves of $Ru(bpy)_3^{2+}$ with and without TPA were less significant, which may be interpreted in terms of an electrocatalytic reaction mechanism. Khramov and Collinson[25] have also observed a similar phenomenon with $Ru(bpy)_3^{2+}$ ion-exchanged in a 67% Nafion–silica composite film.

The corresponding ECL intensity–potential (I_{ECL}–E) curve obtained with the PMT biased at 700 V is shown in Fig. 3B. The onset of luminescence occurred near 0.9–1.0 V, which was consistent with the oxidation of the immobilized $Ru(bpy)_3^{2+}$, and then the ECL intensity rose steeply. The I_{ECL}–E curve became wider as the scan rate was decreased, while the ECL peak intensity stayed relatively constant over the range 10–100 mV s^{-1}. The dependence of the I_{ECL}–E curve on the scan rate was probably due to the slow rate of homogeneous charge transport through the film, since the charge transport diffusion

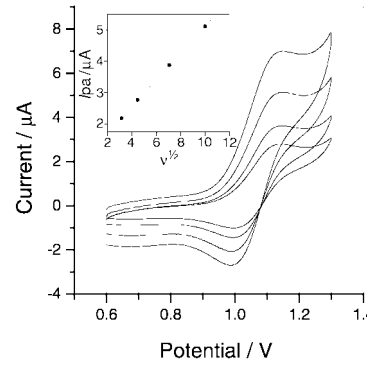

Fig. 2 Cyclic voltammograms of the surface-confined $Ru(bpy)_3^{2+}$ at various scan rates (from inner to outer curve: 10, 20, 50, 100 mV s^{-1}) in 0.1 mol L^{-1} phosphate buffer (pH 7.0). Inset: Relationship between the peak current and the scan rate.

coefficient of $Ru(bpy)_3^{2+}$ immobilized in a 50% PSS–silica composite film was estimated to be 2.8×10^{-10} cm^2 s^{-1}. Since the ECL emission of the system probably arose from the energetic electron-transfer reduction between the electrogenerated $Ru(bpy)_3^{3+}$ and the deprotonated TPA radical ($TPA^{\bullet}$) in the film, the ECL reaction of $Ru(bpy)_3^{2+}$ with TPA can be expressed as follows:[12,13]

$$Ru(bpy)_3^{2+} \rightarrow Ru(bpy)_3^{3+} + e^- \quad (1)$$

$$TPA \rightarrow TPA^{+\bullet} + e^- \quad (2)$$

$$TPA^{+\bullet} \rightarrow TPA^{\bullet} + H^+ \quad (3)$$

$$Ru(bpy)_3^{3+} + TPA^{\bullet} \rightarrow [Ru(bpy)_3^{2+}]^* \quad (4)$$

$$[Ru(bpy)_3^{2+}]^* \rightarrow Ru(bpy)_3^{2+} + h\nu \quad (5)$$

As a control, Fig. 4A shows the CVs of $Ru(bpy)_3^{2+}$ immobilized in a pure silica film at 10 mV s^{-1} with and without TPA in 0.1 mol L^{-1} phosphate buffer (pH 7.0). The corresponding I_{ECL}–E curve is shown in Fig. 4B. The anodic current only increased slightly in the presence of TPA, which was in sharp contrast to that observed at the PSS–silica composite films. The differences between the CVs of $Ru(bpy)_3^{2+}$ in the presence and absence of TPA were not as obvious as those observed at the PSS–silica composite films, and the ECL peak intensity was much lower than that obtained at the PSS–silica composite films.

Effect of PSS

The effect of the PSS content in the composite films on the ECL intensity is shown in Fig. 5. In this plot, the ECL intensity was obtained by using the peak intensity on the I_{ECL}–E curves acquired at 10 mV s^{-1}. The ECL intensity increased rapidly as the PSS content increased. The peak intensity observed at a 33.3% PSS–silica film was *ca*. 20-fold higher than that observed at a pure silica film, although these materials contain the same amount of $Ru(bpy)_3^{2+}$. However, the ECL intensity was considerably smaller for films containing high concentrations of Nafion.[25] The larger ECL obtained at the PSS–silica films could be attributed to the presence of PSS which may enhance the ECL of $Ru(bpy)_3^{2+}$, while it is reported that PSS can markedly enhance the excimer formation of bis(α-naphthylmethyl)ammonium chloride and (α-naphthylmethyl)-ammonium chloride.[30] However, on increasing the PSS content further, the ECL intensity decreased, which may be because, at a high content of PSS, the microstructure of PSS dominates the physical and chemical properties of the film, as the charge transport diffusion coefficient decreased at a high content of PSS. The content of PSS also affects the shape of the CV curve. With PSS, the differences between the CVs of $Ru(bpy)_3^{2+}$ in the presence and absence of TPA were more significant compared with those observed at the pure silica films.

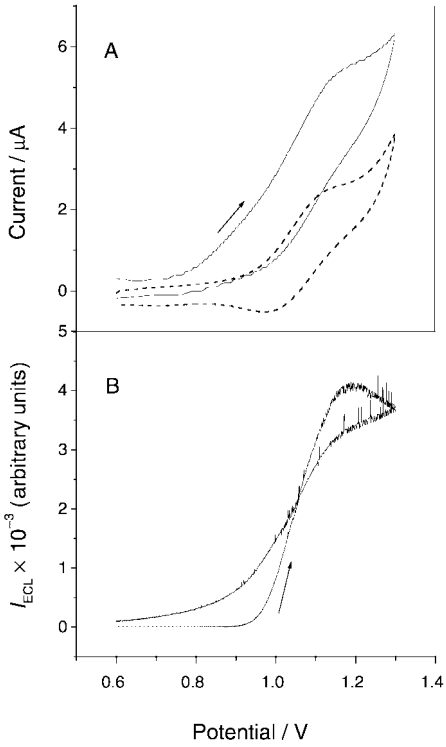

Fig. 3 (A) Cyclic voltammograms of $Ru(bpy)_3^{2+}$ immobilized in 50% PSS–silica composite film in 0.1 mol L^{-1} phosphate buffer (pH 7.0) with (solid line) and without (broken line) 1 mmol L^{-1} TPA. Scan rate: 10 mV s^{-1}. (B) The corresponding I_{ECL}–E curve for PSS–silica immobilized $Ru(bpy)_3^{2+}$ in 1 mmol L^{-1} TPA.

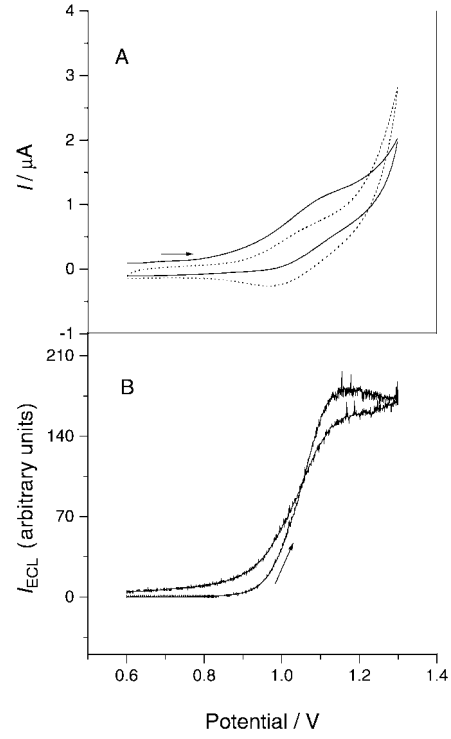

Fig. 4 (A) Cyclic voltammograms of $Ru(bpy)_3^{2+}$ immobilized in pure silica film in 0.1 mol L^{-1} phosphate buffer (pH 7.0) with (solid line) and without (broken line) 1 mmol L^{-1} TPA. Scan rate: 10 mV s^{-1}. (B) The corresponding I_{ECL}–E curve for pure silica immobilized $Ru(bpy)_3^{2+}$ in 1 mmol L^{-1} TPA.

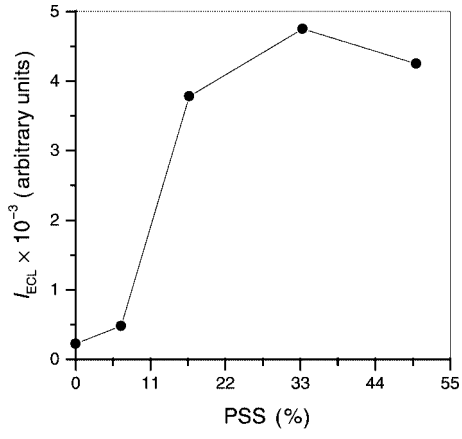

Fig. 5 Dependence of ECL peak intensity on the content of PSS incorporated into the composite films. The ECL intensity was obtained by using the peak value on the I_{ECL}–E curves acquired at 10 mV s^{-1}.

Effect of potential and pH

In order to characterize the sensitivity of the modified electrode, it is of interest to examine the impact of sample pH and potential on the ECL responses. In this work, we investigated the effect of pH and potential on the ECL emission of the $Ru(bpy)_3^{2+}$-modified electrode in solutions containing oxalate and TPA, respectively, in an FIA system. The flow rate was 1.27 mL min^{-1} and the sample injections were made every 1 min for both oxalate and TPA. Concentrations used for oxalate and TPA were both 1 mmol L^{-1}.

To obtain ECL, the potential was stepped from 0 to positive values. The ECL intensity obtained from solutions containing oxalate reached a maximum at 1.1 V, then began to decrease when the applied potential became more positive. The maximum ECL intensity for TPA was obtained at a potential of 1.2 V. In order to obtain good reproducibility and sensitivity, subsequent experiments were conducted by stepping the potential from 0 to 1.1 V for oxalate and from 0 to 1.2 V for TPA.

For pH studies, 0.1 mol L^{-1} phosphate buffer was used to prepare samples at pH values ranging from 3 to 9. A previous study had shown that the ECL of $Ru(bpy)_3^{2+}$/Nafion was not affected by the pH.[9] In contrast to the previous results, the ECL of $Ru(bpy)_3^{2+}$ immobilized in PSS–silica composite films with oxalate and TPA showed a marked dependence on pH. The ECL peak intensity for oxalate reached a maximum value at pH 6.0. The ECL emission of TPA increased on increasing the pH from 3 to 7, then decreased at pH values higher than 8. This was similar to the results at Nafion–silica composite films.[25] The strong pH dependence of the ECL suggested that the deprotonation of TPA ($pK_a = 10.7$) was required for efficient ECL in these composite films, which was consistent with the mechanism proposed for solution-based ECL with TPA [eqn. (1)–(5)].[12,13,25] For oxalate, the ECL reaction with $Ru(bpy)_3^{2+}$ can be expressed by eqn. (6)–(10).[8] At lower pH values the predominant species in solution was $HC_2O_4^-$ (for oxalic acid, $pK_{a_1} = 1.23$, $pK_{a_2} = 4.19$), which underwent a reaction sequence similar to that represented by eqn. (6)–(10) with the reactive intermediate now being $CO_2H^{\bullet}$, a much weaker reducing agent than $CO_2^{\bullet -}$. This would account for the pH dependence of oxalate.[8]

$$Ru(bpy)_3^{2+} \rightarrow Ru(bpy)_3^{3+} + e^- \quad (6)$$

$$Ru(bpy)_3^{3+} + C_2O_4^{2-} \rightarrow Ru(bpy)_3^{2+} + C_2O_4^{\bullet -} \quad (7)$$

$$C_2O_4^{\bullet -} \rightarrow CO_2^{\bullet -} + CO_2 \quad (8)$$

$$Ru(bpy)_3^{3+} + CO_2^{\bullet -} \rightarrow [Ru(bpy)_3^{2+}]^* \quad (9)$$

$$[Ru(bpy)_3^{2+}]^* \rightarrow Ru(bpy)_3^{2+} + h\nu \quad (10)$$

Determination of oxalate, TPA and NADH

The $Ru(bpy)_3^{2+}$/Nafion electrodes used to determine oxalate, TPA and NADH show high sensitivity and function over a wide pH range. However, the disadvantages of this film are obvious, including reorganization of the film over time, day-to-day instability of the film and the irreproducibility between film preparation.[9] In our experiments, in order to evaluate the sensitivity of the silica composite film modified electrode, we have also used $Ru(bpy)_3^{2+}$ immobilized in 16.7% PSS–silica composite films to determine the three analytes mentioned above in a flowing system. The carrier stream was 0.1 mol L^{-1} phosphate buffer (pH 6.0 for oxalate and pH 7.0 for TPA and NADH). The applied potential was set at 1.1 V for oxalate and at 1.2 V for TPA and NADH. Sample injections were made every 1 min, which was twice the rate of that in a previous study,[9] indicating that the modified electrode showed a fast response which was due to the fast diffusion of the analytes through the composite films in the FIA system.

Table 1 illustrates the figures of merit for a typical log–log calibration plot of ECL peak intensity *versus* the concentration of oxalate, TPA, and NADH. The ECL intensity increased linearly with the concentration of oxalate over the concentration range 0.001–1 mmol L^{-1} (intercept: 2.37, correlation coefficient: 0.998) with a detection limit of 0.1 μmol L^{-1}. Peak intensities showed good reproducibility (as shown in Fig. 6), yielding a precision of 2.4% for repetitive measurements (n = 5). The linear range was consistent with the investigations of solution-phase ECL detection.[7,8]

TPA has proved to be the most efficient amine for the $Ru(bpy)_3^{2+}$ ECL reaction due to its structural attributes.[31] The ECL intensity was proportional to the TPA concentration in the range 0.001–1 mmol L^{-1} (intercept: 2.68, correlation coefficient: 0.998) with a detection limit of 0.1 μmol L^{-1}. ECL peak heights showed good reproducibility, with a precision of 3.9% for repetitive measurements (n = 5).

NADH is a coenzyme distributed widely in living organisms and many different compounds undergo enzymatic reactions to produce NADH, and such compounds might be detected indirectly *via* the detection of NADH.[10] Among various approaches to NADH detection, ECL detection with $Ru(bpy)_3^{2+}$ is of high sensitivity.[9] In this paper, $Ru(bpy)_3^{2+}$ immobilized in a 16.7% PSS–silica composite film was also used to determine NADH. The ECL intensity increased linearly with the NADH concentration over the concentration range 0.001–1 mmol L^{-1} (intercept: 1.89, correlation coefficient: 0.994), yielding a detection limit of 0.5 μmol L^{-1}. The peak height reproducibility was 0.9% for repetitive injections (n = 5).

Selectivity studies

One of the goals of this work was to develop a sensor capable of determining analyte concentrations in biological matrices (*i.e.* blood and urine). Therefore, experiments were performed to determine the selectivity or to reveal potential analytes in such matrices for immobilized $Ru(bpy)_3^{2+}$. The carrier stream was 0.1 mol L^{-1} phosphate buffer (pH 6.0). All samples were prepared at a concentration of 1 mmol L^{-1} in the same buffer. The following compounds, *viz*., histidine, cystine, alanine, serine, ascorbic acid, threonine, asparagine, arginine, glutamic acid, tyrosine, phenylalanine, lactamine and proline, were tested for ECL emission with the immobilized $Ru(bpy)_3^{2+}$ and the results are listed in Table 2. Oxalate (1 mmol L^{-1}) was used as a reference and injections were made between test compounds in order to monitor any changes in ECL intensity due to system drift. Of all the compounds tested, only proline produced significant ECL intensity. Signals from proline were more than two times greater than those observed for oxalate at the same concentration. Downey and Nieman have also observed ECL for proline with Nafion-immobilized $Ru(bpy)_3^{2+}$.[9]

Stability of immobilized $Ru(bpy)_3^{2+}$

The stability of $Ru(bpy)_3^{2+}$ immobilized in the PSS–silica composite films was tested over a 1 week period. When the

Table 1 Figures of merit for typical log–log calibration graphs for oxalate, TPA and NADH obtained with $Ru(bpy)_3^{2+}$ immobilized in 16.7% PSS-silica composite film. The carrier stream was 0.1 mol L^{-1} phosphate buffer (pH 6.0 for oxalate, pH 7.0 for TPA and NADH); the electrode was poised at 1.1 V for oxalate and 1.2 V for TPA and NADH

Compound	Slope of calibration graph	Linear range/ mmol L^{-1}	RSD (%)[a]	LOD/ mmol L^{-1}
Oxalate	0.39	1×10^{-3}–1	2.4	1×10^{-4}
TPA	0.65	1×10^{-3}–1	3.9	1×10^{-4}
NADH	0.33	1×10^{-3}–1	0.9	5×10^{-4}

[a] n = 5.

modified electrode (16.7% PSS) was stored in the dry state at room temperature, only a 2% decrease in the ECL response to 1 mmol L^{-1} TPA was found over this period. Moreover, when the modified electrode was immersed in phosphate buffer and under a potential cycle, the ECL response remained constant. In contrast, when $Ru(bpy)_3^{2+}$ was immobilized in pure silica, a distinct decrease was observed in a relatively short time when the electrode was cycled due to leaching of the complex.[24] The good stability can be explained as follows: First, $Ru(bpy)_3^{2+}$ is a very stable CL reagent. Second, the hydrogen bond in the film is favorable for preventing $Ru(bpy)_3^{2+}$ from leaching out of the thin film. Triton X-100 has a multi-hydroxyl structure. When it is added to the sol–gel precursor solution, it can form hydrogen bonds with the deprotonated silanol groups and remains in the pores of the film,[32] thus preventing drying fractures of the sol–gel films during gelation and even on repeated wet–dry cycles.[27] Third, the presence of PSS, a type of polyelectrolyte, in the silicates probably makes the silica film adhere strongly to the GCE and sufficiently robust for handling. In previous studies,[33,34] polystyrene was added to the silicates to produce robust films and the porous polystyrene–silicate layers provided good mechanical stability and did not interfere with the diffusion of electroactive species. Fourth, the strong interaction between $Ru(bpy)_3^{2+}$ and PSS leads to the formation of a large ion-association complex, which can avoid $Ru(bpy)_3^{2+}$ leaching out of the silica matrix. Finally, some cooperation may exist between PSS, Triton X-100, and silica.

Conclusions

The combination of PSS, Triton X-100, and silica sol provides an effective means to prepare composite films for the direct immobilization of the ECL reagent, $Ru(bpy)_3^{2+}$. The immobilization eliminates the need to deliver the ECL reagent to the reaction zone continuously and minimizes the amount of reagent consumed.[9] The cyclic voltammetry and ECL of $Ru(bpy)_3^{2+}$ immobilized in PSS–silica composite films have been investigated with the $Ru(bpy)_3^{2+}$–TPA system. Both the electrochemical and ECL behavior of the immobilized $Ru(bpy)_3^{2+}$ were found to be strongly dependent on the content of PSS. The presence of PSS can greatly enhance the ECL intensity. The composite film modified electrode was used to detect oxalate, TPA, and NADH in an FIA system and exhibited a variety of good performance characteristics including high sensitivity, short response time and good stability. These results suggest that the proposed modification methods may hold promise in ECL detection, and the composite film may serve as an alternative material for the immobilization of other reagents.

In addition, the structure of the flow cell developed is very simple. It can be used not only in ECL detection, but also in electrochemical detection since the structure of the cell is much simpler than that of other electrochemical flow cells. This indicates that the flow cell will find wide application.

Table 2 ECL intensities observed for compounds in selectivity study with PMT biased at 700 V

Compound	ECL intensity (arbitrary units)	Compound	ECL intensities (arbitrary units)
TPA	4300	Threonine	2
Oxalate	350	Asparagine	5
NADH	76	Arginine	44
Histidine	17	Glutamic acid	0
Cystine	0	Tyrosine	7
Alanine	0	Phenylalanine	9
Serine	0	Lactamine	16
Ascorbic acid	0	Proline	784

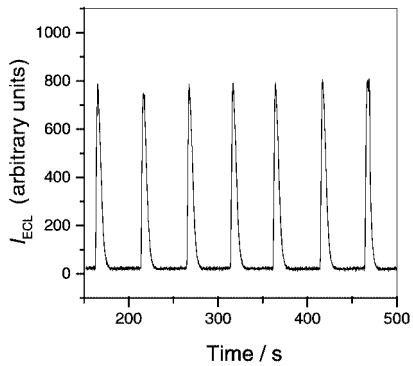

Fig. 6 ECL emission from $Ru(bpy)_3^{2+}$ immobilized in 16.7% PSS–silica composite film in FIA for seven consecutive injections of 1 mmol L^{-1} oxalate. The carrier stream was 0.1 mol L^{-1} phosphate buffer (pH 6.0). The potential was poised at 1.1 V. The flow rate was 1.27 mL min^{-1}.

Acknowledgements

The support of this research by the National Natural Science Foundation of China (Grant No. 29835120) is gratefully acknowledged.

References

1 N. E. Tokel and A. J. Bard, *J. Am. Chem. Soc.*, 1972, **94**, 2862.
2 M. M. Chang, T. Saji and A. J. Bard, *J. Am. Chem. Soc.*, 1977, **99**, 5339.
3 M. M. Collinson, P. Pastore, K. M. Maness and R. W. Wightman, *J. Am. Chem. Soc.*, 1994, **116**, 4095.
4 K. M. Maness, H. Masui, R. W. Wightman and R. W. Murray, *J. Am. Chem. Soc.*, 1997, **119**, 3987.
5 A. W. Knight, *Trends Anal. Chem.*, 1999, **18**, 47.
6 R. D. Gerardi, N. W. Barnett and S. W. Lewis, *Anal. Chim. Acta*, 1999, **378**, 1.
7 I. Rubinstein, C. R. Martin and A. J. Bard, *Anal. Chem.*, 1983, **55**, 1580.
8 I. Rubinstein and A. J. Bard, *J. Am. Chem. Soc.*, 1981, **103**, 512.
9 T. M. Downey and T. A. Nieman, *Anal. Chem.*, 1992, **64**, 261.
10 A. F. Martin and T. A. Nieman, *Anal. Chim. Acta*, 1993, **281**, 475.
11 J. B. Noffsinger and N. D. Danielson, *Anal. Chem.*, 1987, **59**, 865.
12 J. K. Leland and M. J. Powell, *J. Electrochem. Soc.*, 1990, **137**, 3127.
13 F. Kanoufi and A. J. Bard, *J. Phys. Chem.*, 1999, **103**, 10 469.
14 L. He, K. A. Cox and N. D. Danielson, *Anal. Lett.*, 1990, **23**, 195.
15 W. A. Jackson and D. R. Bobbitt, *Anal. Chim. Acta*, 1994, **285**, 309.
16 L. L. Shultz, J. S. Stoyanoff and T. A. Nieman, *Anal. Chem.*, 1996, **68**, 349.
17 X. Zhang and A. J. Bard, *J. Phys. Chem.*, 1988, **92**, 5566.
18 C. J. Miller, P. McCord and A. J. Bard, *Langmuir*, 1991, **7**, 2781.
19 Y. S. Obeng and A. J. Bard, *Langmuir*, 1991, **7**, 195.
20 Y. Sato and K. Uosaki, *J. Electroanal. Chem.*, 1995, **384**, 57.
21 B. C. Dave, B. Dunn, J. S. Valentine and J. I. Zink, *Anal. Chem.*, 1994, **66**, 1120A.
22 D. Levy, *Chem. Mater.*, 1997, **9**, 2666.
23 D. Avnir, *Acc. Chem. Res.*, 1995, **28**, 328.
24 O. Dvorak and K. M. DeArmond, *J. Phys. Chem.*, 1993, **97**, 2646.
25 A. N. Khramov and M. M. Collinson, *Anal. Chem.*, 2000, **72**, 2943.
26 Y. Shi and C. J . Seliskar, *Chem. Mater.*, 1997, **9**, 821.
27 O. Lev, M. Tsionsky, L. Rabinovich, V. Glezer, S. Sampath, I. Pankratov and J. Gun, *Anal. Chem.*, 1995, **67**, 22A.
28 G. Xu and S. Dong, *Analyst*, 1999, **124**, 1085.
29 B. Wang, B. Li, Z. Wang, G. Xu, Q. Wang and S. Dong, *Anal. Chem.*, 1999, **71**, 1935.
30 N. J. Turro, T. Okubo, C. Chung, J. Emert and R. Catena, *J. Am. Chem. Soc.*, 1982, **104**, 4799.
31 A. W. Knight and G. M. Greenway, *Analyst*, 1996, **121**, 101R.
32 W. Song, Y. Liu, N. Lu, H. Xu and C. Sun, *Electrochim. Acta*, 2000, **45**, 1639.
33 M. Sykora and J. Meyer, *Chem. Mater.*, 1999, **11**, 1186.
34 G. Villemure and T. J. Pinnavaia, *Chem. Mater.*, 1999, **11**, 789.